

Highly Efficient Bacteria Filtration and Total Elimination by Novel Metal-Graphene Nanoribbons

Duong Thai^a, Phuong Nam Ngoc Le^b, Tung Quang Ho^b, Linh Khanh Nguyen^a, Truc Thanh Thi Do^a, Thang Xuan Trinh^a, Thien Huynh Ngo^a, Doanh Tu Tieu^{a,*}

^aResearch Laboratories of Saigon Hi-Tech Park, Lot I3, N2 Road, Thu Duc City, Ho Chi Minh City, 70000, Viet Nam

^bTran Dai Nghia High School for the Gifted, 20 Ly Tu Trong Street, Ben Nghe Ward, Ho Chi Minh City, 70000, Viet Nam
 Doanh.tietu@shtplabs.org

Environmental pollution has recently become one of the most essential issues and has received critical attention in the world. Both fine dust particles and airborne bacteria can penetrate the human body, causing diseases of the respiratory system and blood circulatory system. A filter membrane is capable of both filtering ultrafine dust and destroying bacteria that have been investigated. Graphene nanoribbons (GNRs) were synthesized from the multi-walled carbon nanotubes (CNTs) by the unzipping method. Various densities of GNRs were coated on the porous stainless steel (PSS) via the vacuum filtration process. The structure of GNRs coating on the porous stainless steel was characterized by field emission scanning electron microscopy (SEM) and energy-dispersive X-ray spectroscopy (EDX). The filter membrane was analyzed for their air resistance based on the pressure drop-air flow and showed the filtration efficiency of fine dust particles greater than 99%. The ability of this membrane to filter and destroy bacteria was demonstrated with a 6 A current and low voltage under 3 V in a short time of under 1 minute. The results indicated that the GNRs coated on PSS have high potential as filter membranes due to their efficiency and commercial ability for large-scale production for applications in various fields such as air purifiers, biomedicine, food processing, and water treatment.

1. Introduction

Air pollution issues have been a hot topic and are causing serious impacts globally. According to the World Health Organization (WHO), nearly 90% of the global population lives in places where air pollution levels exceed air quality guidelines. Fine dust particles of PM₁₀ and PM_{2.5} from exhaust sources at high concentrations significantly pollute the air environment. The fine particle pollutants in the air, especially particles with an aerodynamic diameter smaller than 2.5 μm (PM_{2.5}), are the main causes of cancer, fibrosis, and chronic lung disease. Their contamination with heavy metal components, i.e., cadmium, arsenic, lead, and zinc, increases the negative effects on human health (Gilmour et al., 1996; Na et al., 2014). Therefore, air quality management and air pollution filtration have been of interest to experts in various fields, aiming to minimize and eliminate negative effects on the environment and humans. PM particles smaller than 10 μm (PM₁₀) can be deposited in the lungs, and PM_{2.5} can penetrate the blood vessels where they can cause serious effects on the circulatory and respiratory systems (Arden et al., 2002).

Besides, the polluting fine particles in the atmosphere also contain various microorganisms, such as *Streptococcus pyogenes*, *Mycobacterium tuberculosis*, *Bordetella pertussis*, and adenovirus, which increase the risk level of airborne infections. During the COVID-19 pandemic, researchers have found that the coronavirus can survive up to three hours in the air and access directly to the airways and lungs. An increase in PM_{2.5} density of only 1 μg/m³ can increase the mortality rate of COVID-19 by 8% (Wu et al., 2020). These bacteria and viruses are mainly transmitted between people through the air and affect the respiratory system of patients, impacting the lives of millions of people around the world. This is an urgent issue that needs to be addressed. Materials that can effectively block atmospheric pollution, such as PM_{2.5}, and kill bacteria and viruses will be of vital importance in the fight to reduce such contamination.

Graphene is known as the material of the 21st century with many outstanding features, such as a large surface area of $2630 \text{ m}^2\cdot\text{g}^{-1}$, Young's modulus 0.5–1 TPa, a tensile strength of 125 GPa (Park et al., 2009), electron mobility of $2.5 \times 10^5 \text{ cm}^2\cdot\text{V}^{-1}\cdot\text{s}^{-1}$ (Novoselov et al., 2012), which generated a high electron current when charging with a low voltage. Furthermore, when some bacteria come in contact with the graphene matrix, strong binding is formed between the functional group of the graphene and their cell membrane. The reactive oxygen species (ROS) was generated from this bond, causing the deoxyribonucleic acid (DNA) to condense and physically damage the cell membrane (Krishnamoorthy et al., 2012). Some mechanisms were proposed to demonstrate the antibacterial ability of graphene material. The result (Akhavan et al., 2010) reported that graphene can break cell membranes due to the sharp edge when the bacteria was in direct contact, while some functional groups in the basal plane of graphene can bind lipids or proteins of the membrane and deactivate bacteria (Hui et al., 2014). The research (Ye et al., 2021) used the electrical stimulus to effectively disrupt the electron transport of the bacterial respiratory chain, causing a burst of respiratory byproducts of ROS and leading to the death of the bacterial cells. Therefore, graphene material became a promising material for antibacterial application.

Graphene was widely investigated as antibacterial air filter membranes. The traditional fibrous filter, including glass fibers, melt-blown fibers (Feng et al., 2013), or electrospun fibers from polymers (Xu et al., 2016), showed the ability to capture fine dust while maintaining the air permeability. To kill bacteria in the air, some antibacterial materials, such as graphene (Antony et al., 2020), or nano noble metal (Qinghong et al., 2024), were coated on the fibers of the filter. However, the structural stability could not be sustained for a long time because of the inferior cross-linking of the materials. To improve the stability of graphene–polymer composite, laser-induced graphene on a polyimide substrate proved its ability to kill bacteria when charged with a voltage of roughly 15 volts. The high voltage during this process has its own drawback; a temperature over 300°C was generated while charging at 15 volts, making the method unfit for commercial filtration (Michaelet al., 2019). Nanoribbons of structured graphene were unzipped from carbon nanotubes with a small diameter of less than 50 nm and a large length of approximately $50 \mu\text{m}$, which could be interwoven to form a membrane with a tiny pore structure. The addition of such a structure is its good electrical conductivity, allowing the graphene nanoribbons filter to eliminate bacteria with a low voltage (Duong et al., 2021).

In this study, graphene nanoribbons were fabricated from multi-walled carbon nanotubes (CNTs) by the unzipping method and then deposited on stainless-steel substrates to create metal-carbon filter membranes. The density of graphene nanoribbons was investigated for two goals: 1) Firstly, to determine the amount of graphene nanoribbons needed to cover the pore of the stainless-steel mesh and reduce the pore size of the filter. 2) Secondly, we sought to decrease the resistance of the new filter to enhance the ability to terminate bacteria at lower voltages.

2. Materials and methods

2.1 Materials

Carbon nanotubes (CNTs) was supplied by NTherma Corp, USA. Potassium permanganate (KMnO_4 , Sigma-Aldrich, $\geq 99\%$), sulfuric acid (H_2SO_4 99.999 %, Sigma-Aldrich), hydrogen peroxide (H_2O_2 , 50 %, Solvay, Thailand), ethanol 96° ($\text{C}_2\text{H}_5\text{OH}$, Vietnam), and stainless-steel mesh (500 mesh) were used.

2.2 Methods

Fabrication of graphene nanoribbons from carbon nanotubes

Graphene nanoribbons were fabricated from the delamination of multiwall CNTs chemically using strong oxidation agents in the acid environment. 1.75 g of multiwall CNTs and 8.75 g of KMnO_4 were stirred in 300 ml H_2SO_4 at room temperature for 30 minutes before increasing the temperature to 100°C for 45 minutes as in our previous research (Tieu et al., 2020). After cooling in the ice bath, 5 ml of H_2O_2 was added. The precipitation was filtered and washed extensively with deionized water and followed by drying at 100°C in the vacuum oven to produce the desired graphene nanoribbons powder.

Fabrication of graphene nanoribbons coated onto stainless-steel

The process of fabricating graphene nanoribbons coating on a stainless-steel substrate via the vacuum filtration method was described in Figure 1.

GNRs were slowly dispersed in an isopropyl alcohol (IPA) solution and kept at a constant 0.1% concentration. The various densities of GNRs onto the PSS substrate from 0.1 to 0.4 mg/cm^2 were investigated and named GS0.1, GS0.2, GS0.3, and GS0.4, respectively. The solution was put into an ice bath to avoid the increasing temperature during the probe-sonication. All the experiments were carried out for 15 minutes with 70% sonication amplitude. The uniform solution was slowly poured into the vacuum filtration system containing the

stainless-steel mesh. Finally, the GNRs-coated stainless-steel sample was dried in the vacuum oven at 80°C for 30 minutes.

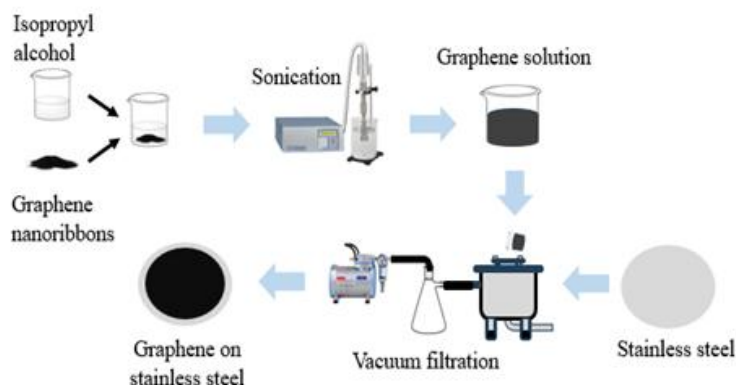


Figure 1: Schematic diagram of Graphene Nanoribbons filter formation process on the stainless-steel substrate

2.3 Characterization

The structural characterization of graphene nanoribbons coated stainless-steel was obtained by scanning electron microscopy (FESEM S4800, Hitachi, Japan) and Energy Dispersive X-ray Spectrum (EDX H-7593, Horiba, England). The filter efficiency was measured by the facemask test equipment (AFT-14, Fayuan Instrument, China). The antibacterial elimination by low voltage was analyzed by DC power supply equipment (ODP3063, OWON, China).

3. Results and discussion

The difference in the structure of the stainless-steel mesh without and with covering by GNRs is shown in Figure 2. When the filter membrane was observed at low magnification by the digital image, the silver color of the stainless-steel mesh was changed to black by the presence of GNRs (Figure 2a and Figure 2c, respectively). The image of the uniform structure of the stainless-steel mesh before and after coating by GNRs is captured in the FE SEM image at high magnification. The structure of the stainless-steel mesh with the pore size of about 30 μm was woven by the diameter of 20 μm wires in Figure 2b. The nano-diameter ribbons were interwoven with each other, creating a membrane onto PSS in Figure 2d, and the inset image indicated the GNRs matrices with pores of around 100 nm. The GNRs completely covered and reduced the pore size of the stainless-steel mesh, demonstrating the ability to capture dust particles as well as bacteria in the air.

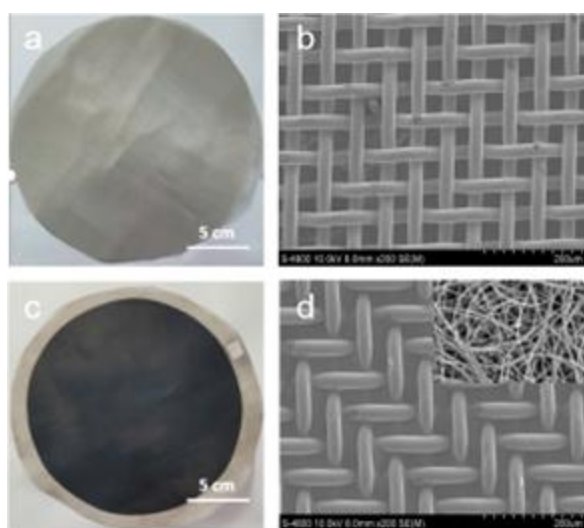


Figure 2: Uncoated and GNRs-coated onto stainless-steel substrate (a,c) digital images and (b,d) FE - SEM images

The EDX spectrum showed that there was only carbon material, i.e., GNRs were deposited onto the surface of the metal with no other impurities (Figure 3a).

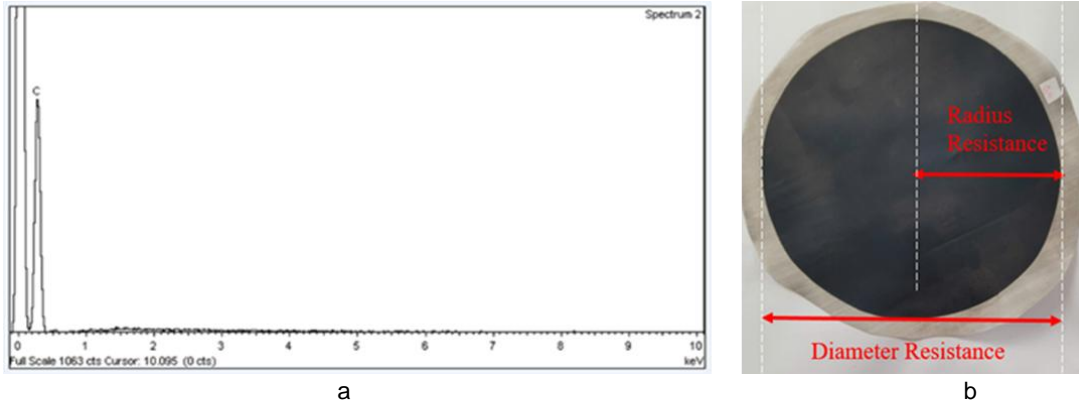


Figure 3: (a) The EDX spectrum of graphene nanoribbons coated on stainless-steel mesh, (b) Illustration of the radius resistance and diameter resistance

The electrical resistance of graphene nanoribbons-coated stainless-steel samples was measured by a multimeter. The distance (cm) between the two points of the multimeter was respectively the radius and the diameter of the circle sample called radius resistance and diameter resistance (Ω) in Figure 3b.

The electrical resistances of the filter membrane with different densities of GNRs (from 0.1 mg/cm² to 0.4 mg/cm²) are shown in Table 1. The results indicated that the resistance of the membrane and the density of GNRs on the stainless-steel mesh varied linearly. The resistance increases from 1.80 Ω , 2.45 Ω , 2.90 Ω , and 4.95 Ω corresponding to the density of GNRs from 0.1, 0.2, 0.3, and 0.4 mg/cm². Moreover, the resistance measured at the radius and the diameter positions of the membrane were negligibly different, proving the ability to completely cover GNRs on stainless-steel mesh. The resistance of the GNRs on stainless-steel mesh was under 5 Ω and lower than that of GNRs in the previous study (Duong et al., 2021). The applied amount of GNRs was enough to coat the stainless steel with a thin layer.

Table 1: The electrical resistance of the GNRs coated onto stainless steel with various densities

No.Sample	Density of GNRs (mg/cm ²)	Radius Resistance (Ω)	Diameter Resistance (Ω)	Average Resistance (Ω)
1 SS	0	1.0 \pm 0.16	0.9 \pm 0.16	0.95
2 GS0.1	0.1	1.9 \pm 0.21	1.7 \pm 0.26	1.80
3 GS0.2	0.2	2.4 \pm 0.25	2.5 \pm 0.21	2.45
4 GS0.3	0.3	2.8 \pm 0.15	3.0 \pm 0.26	2.90
5 GS0.4	0.4	5.0 \pm 0.25	4.9 \pm 0.3	4.95

The effective fine dust filtration of GNRs onto stainless steel mesh is shown in Table 2. The large pore size of the stainless steel was unable to capture fine dust with a low filtration efficiency of approximately 10%. When the stainless-steel mesh was covered by graphene nanoribbons, the dust filtration efficiency was increased significantly. With the low density of graphene content on the mesh at 0.1 and 0.2 mg/cm², the dust filtration efficiencies were only 81.5376% and 93.2442%, respectively. The filtration efficiency reached over 99% and did not change significantly with the higher content from GS0.3 to GS0.4 samples. The results indicated that the density of GNRs over 0.3 mg/cm² was enough to completely cover the pores of the stainless-steel mesh, thereby achieving the desired dust filtration efficiency of 99%.

Table 2: Filtration efficiency testing with the various densities of GNRs

No.Sample	Aerosol type	Flow (L/minute)	Resistance (Pa)	Upstream (mg/m ³)	Downstream (mg/m ³)	PFE (%)
1 SS	NaCl	4.5	34.13	7.204	6.390	10.5523
2 GS0.1	NaCl	4.5	428.85	7.232	1.320	81.5376
3 GS0.2	NaCl	4.4	629.01	7.468	0.441	93.2442
4 GS0.3	NaCl	4.5	896.12	8.985	0.078	99.1165
5 GS0.4	NaCl	4.3	921.37	8.844	0.063	99.2875

In addition to the dust filtration efficiency, the resistance of the filter membrane while the air flows through the membrane is another important factor. The results of Table 2 indicated that the resistance value and the density of graphene nanoribbons were a proportional relationship due to the resistance of the membrane increasing with the higher graphene content. Specifically, the impedance value increases from 428.85 Pa, 629.01 Pa, 896.12 Pa, and 921.37 Pa when the density of GNRs was increased from 0.1, 0.2, 0.3, and 0.4 mg/cm², respectively. The high resistance value indicated the difficulty of the airflow was hard to permeate the filter membrane and directly influenced the dust filtration efficiency. Although the same dust filter efficiency was over 99%, the GS0.3 sample proved to be a more ideal filter membrane due to the lower resistance compared to the GS0.4 sample. The value pressure resistance of the GS0.3 sample filter membrane is 896.12 Pa, smaller than the 921.37 Pa of the GS0.4 sample; therefore, the density of 0.3 mg/cm² was more suitable for the antibacterial filtration membrane with low voltage.

The density of graphene nanoribbons on stainless steel at 0.3 mg/cm² was chosen to be tested for the elimination of bacteria at low voltage for 30 seconds (Table 3). The current value was varied while the voltage was measured by the DC supplier.

Table 3: The ability to destroy E.Coli bacteria with various currents

No.	Density of GNRs	Time (second)	I (A)	U (V)
1	0.3	30	3	1,234
2	0.3	30	4	1,669
3	0.3	30	5	2,099
4	0.3	30	6	2,440

The effect of increasing current through the graphene nanoribbons-coated mesh on bacteria with low voltage is shown by FE-SEM images in Figure 4.

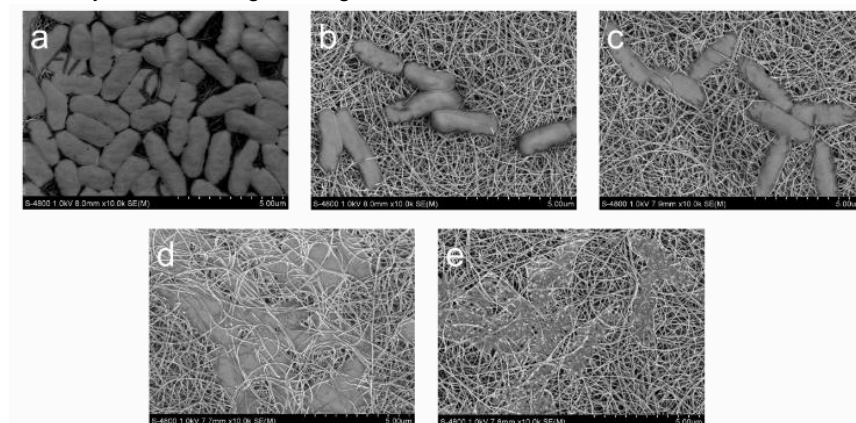


Figure 4: The ability to kill E.Coli bacteria with the various currents a) 0 A, b) 3 A, c) 4 A, d) 5 A, and e) 6 A

Before a current was applied, the *E. coli* bacteria structure was an oval shape with a size of about 2–4 μm . When the electric current is less than or equal to 3 A, the shape of *E. coli* bacteria was barely changed (Figure 4a,b). At the electric current of 4 A, some cuts in the cell membrane appeared at the contact sites with the graphene nanoribbons (Figure 4c). The cell membrane was completely broken, and only an amorphous shape was observed at the current of 5 A (Figure 4d). When the current was increased to 6 A, the result showed the full elimination of *E. coli* bacteria at a low voltage of 2.4 volts (Figure 4e), surpassing the previous investigations (Michael et al., 2019). While a few-layer graphene coating on a porous network of a ZnO filter can filter > 99.9% of even the most penetrating particles ($d = 300 \text{ nm}$) and is capable of capturing > 95% of microorganisms at Joule heating 300°C (Armin et al., 2023). This result can compare the zein nanofibers (zNFs) as the upper layer on anchored Ag nanoparticles (NPs) on paper towel (PT), i.e., the zNFs-Ag@PT air filter structure, which can inhibit the *Candida albicans* (yeast), *Micrococcus luteus* (Gram-positive bacteria), and *E. coli* (Gram-negative bacteria) and show the excellent particle filtration performance with 99.3% efficiency for PM0.3 (Xin et al., 2021). The electrical resistance of graphene nanoribbons coated with stainless steel was lower than that of the graphene membrane, which generated a high electron current when charged with a smaller voltage, which can eliminate the bacteria. Therefore, the GNRs/PSS structure showed both excellent, efficient filtration and antibacterial performance.

4. Conclusion

In this study, graphene nanoribbons were synthesized from carbon nanotubes and used to cover the stainless-steel mesh for membrane filter application. At the density of 0.3 mg/cm² graphene nanoribbons, a high filter efficiency of over 99 % was achieved and the E.coli bacteria was entirely eliminated when a current of 6 A at low voltage under 3 V was applied. The easy scale-up process to fabricate such materials offers high potential for product commercialization of GNRs coated on stainless-steel and their extended applications in various fields such as air purifiers, biomedical, food processing, and water treatment.

Acknowledgments

This research is funded by Saigon HiTech Park Labs, under grant number NVTXTCN 6/2023.

References

- Akhavan O., Ghaderi E., 2010, Toxicity of Graphene and Graphene Oxide Nanowalls against Bacteria, *ACS Nano* 2010, 4, 5731-5736.
- Armin Reimers, Ala Bouhanguel, Erik Greve, Morten Möller, Lena Marie Saure, Sören Kaps, Lasse Wegner, Ali Shaygan Nia, Xinliang Feng, Fabian Schütt, Yves Andres, Rainer Adelung, 2023, Multifunctional, self-cleaning air filters based on graphene-enhanced ceramic networks, *Device*, vol. 1, issue. 4, 100098.
- Antony B.A., Miguel P.V., Clemente L.C., Adolfo L.R.T., Angélica M.M., 2020, Highly Porous Reduced Graphene Oxide-Coated Carbonized Cotton Fibers as Supercapacitor Electrodes, *ACS Omega*, 5, 50, 32149–32159.
- Arden P., Richard T.B., Michael J.T., 2002, Lung cancer, cardiopulmonary mortality, and long-term exposure to fine particulate air pollution, *JAMA*, vol. 287, no. 9, pp. 1132–1141.
- Duong T., Danh N.C., Sinh D.T and Doanh T.T, 2021, The Graphene Nanoribbons based filter membrane for antibacterial application using low applied voltage, *Vietnam Trade and Industry Review*.
- Feng Z., Dawud H. T., Zaifei W., Soondeuk J., Christopher W. M., and Frank S. B., 2013, Nanofibers from Melt Blown Fiber-in-Fiber Polymer Blends, *ACS Macro Letters*, 2, 4, 301–305.
- Gilmour P. S., Brown D. M., Lindsay T. G., Beswick P. H., MacNee W., and Donaldson K., 1996, Adverse health effects of PM10 particles: involvement of iron in generation of hydroxyl radical., *Occup Environ Med*, vol. 53, no. 12, pp. 817–822.
- Hui L., Piao J. G., Auletta J., Hu K., Zhu, Y., Meyer T., Liu, H., Yang L., 2014, Availability of the Basal Planes of Graphene Oxide Determines Whether It Is Antibacterial, *ACS Appl. Mater. Interfaces*, 6, 13183-13190.
- Krishnamoorthy K., Veerapandian M., Zhang, L.H., Yun K., Kim S.J., 2012, Antibacterial Efficiency of Graphene Nanosheets against Pathogenic Bacteria via Lipid Peroxidation, *Phys. Chem. C*, 116, 17280–17287.
- Michael G.S., John T.L., Yuda C., Emily A.M., Anton L., Han X., James M.T, 2019, Self-Sterilizing Laser-Induced Graphene Bacterial Air Filter, *American Chemical Society Nano*, 13 (10), 11912-11920.
- Na W., Zhigao Z., Junlu S., Salem S.A., Jianyong Y., Bin D., 2014, Superamphiphobic nanofibrous membranes for effective filtration of fine particles,” *J Colloid Interface Sci*, vol. 428, pp. 41–48.
- Novoselov K. S., Colombo L., Gellert P. R., Schwab M. G., Kim K., 2012, A roadmap for graphene, *Nature*, vol. 490, no. 7419, pp. 192–200.
- Park S. and Ruoff R. S., 2009, Chemical methods for the production of graphenes, *Nat Nanotechnol*, vol. 4, no. 4, pp. 217–224.
- Qinghong H., Chen M., Mingrui L., Tianyu K., Fangchao Z., Jian R.L., Jiashen L., Yi L., 2024, Hierarchically Porous, Superhydrophobic PLLA/Copper Composite Fibrous Membranes for Air Filtration, *ACS Appl. Polym. Mater*, 6, 2381–2391.
- Tieu Tu Doanh, Thai Duong, Nguyen Cong Danh, Ton Nu Quynh Trang, Ngo Vo Ke Thanh, Vu Thi Hanh Thu, Nguyen Van Cattien, 2020, Highly efficient SERS performance from the silver nanoparticles/graphene nanoribbons/ cellulose paper, vol. 23, no.3, pp 684-693.
- Wu X., Nethery R. C., Sabath M. B., Braun D., Dominici F., 2020, Air pollution and COVID-19 mortality in the United States: Strengths and limitations of an ecological regression analysis, *Sci Adv*, vol. 6, no. 45, pp eabd4049.
- Xin Fan, Lingshuang Rong, Lushi Kong, Yuxin Li, Junrong Huang, Yungang Cao, Wei-Hong Zhong, 2021, Tug-of-war-inspired bio-based air filters with advanced filtration performance, *ACS Appl. Mater. Interfaces*, Vol. 13, Issue. 7, pp 8736-8744
- Xu J., Liu, C., Hsu P.C., Liu K., Zhang R., Liu Y., Cui Y., 2016, Roll-to-roll transfer of electrospun nanofiber film for high-efficiency transparent air filter, *Nano Lett*, 16 (2), 1270–1275.
- Ye W., Yuhui L., Can W., Jiali C., Ning N., Zeyu Y., Yi G., Jieyu Z., Xuefeng H., Yunbing W., 2021, Conductive dual hydrogen bonding hydrogels for the electrical stimulation of infected chronic wounds”, *J. Mater. Chem. B*, 9, 8138.